Imprinted Genes and Hypothalamic Function

AQ1

Michela Pulix [1,2]

Antonius Plagge [1]✉

Email plagge@liverpool.ac.uk

[1] Cellular and Molecular Physiology, Institute of Translational Medicine, University of Liverpool, Liverpool, UK

[2] Department of Neuroscience, Sheffield Institute for Translational Neuroscience, University of Sheffield, Sheffield, UK

Abstract

Genomic imprinting, a specific type of inherited epigenetic regulation, controls a number of genes with important functions in the hypothalamus and its associated neuroendocrinology. Imprinted genes are expressed monoallelically, dependent on the parental origin of the allele, whereby maternally or paternally inherited DNA methylation marks determine gene activity. In this chapter, we provide an overview of imprinted genes with roles in the hypothalamic regulation of whole-body energy homeostasis, neuroendocrine hormone functions, and circadian rhythmicity. As an example for imprinted genes that impact on the central regulation of energy balance, we describe the *Gnas* locus in more detail, since it generates parental allele-specific gene products with antagonistic roles in energy expenditure and sympathetic nervous system activity. Several human neuroendocrine disorders are caused by defects in imprinted genes as described here for Prader–Willi Syndrome and Angelman Syndrome. Furthermore, we outline methodological approaches for the investigation of DNA methylation marks and allelic gene expression, including bisulfite conversion of DNA and pyrosequencing. Recent technological advances to resolve methylation and allelic expression at the single-cell level are introduced.

Keywords

Genomic imprinting
Hypothalamus
Gnas
Energy homeostasis
Prader–Willi syndrome
Angelman syndrome
DNA methylation
Bisulfite conversion of DNA
Pyrosequencing

10.1. Introduction

The term genomic imprinting refers to the expression of certain genes from only one of the two parental

alleles. This is dependent on the parental origin, i.e., some genes are monoallelically expressed from the maternal, others from the paternal allele, while the opposite alleles are silenced. The allelic silencing is already determined in the parental germ cells through epigenetic “marks” and maintained in the somatic tissues of the offspring (Fig. 10.1). To maintain this parent-of-origin-specific gene expression, the epigenetic “marks” are erased in the primordial germline cells of the developing offspring and reset according to the sex of the offspring. This process ensures that the maternal or paternal allelic expression, respectively, of an imprinted gene is inherited from generation to generation. To date, circa 150 imprinted genes have been confirmed in humans and mice, but imprinted gene expression also exists in other mammals (http://www.mousebook.org/imprinting-gene-list; http://igc.otago.ac.nz/home.html). Most imprinted genes occur in conserved clusters, but the imprinting of some genes is species specific.

Fig. 10.1

Inheritance cycle of DNA methylation imprinting marks through the germline and maintenance in somatic tissues. The genomic DNA methylation imprints are established in the germline cells in a sex-specific manner and transmitted to the zygote, where they resist reprogramming events and global changes in DNA methylation, which take place after fertilization. While the genomic imprinting marks are maintained in somatic cells throughout life, they are erased in the primordial germ cells of the developing embryo and re-established de novo according to the sex of the organism, to be transmitted to the next generation. Re-establishment of imprinting marks in gametogenesis occurs prenatally in males and at postnatal stages in females [Adapted from Bartolomei and Ferguson-Smith (2011)]

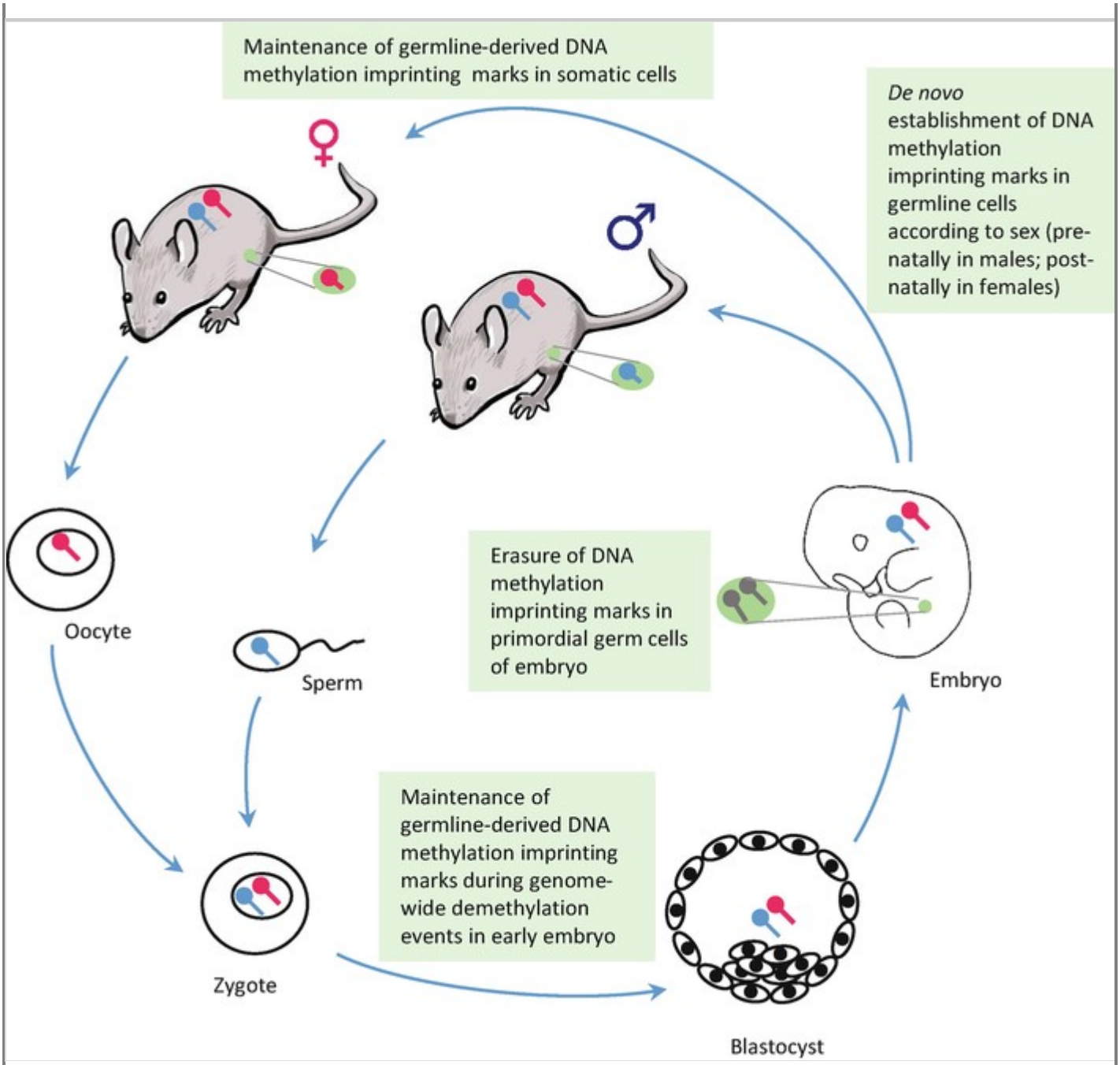

Many imprinted genes have essential roles in embryonic development and placental functions (Plasschaert and Bartolomei 2014). However, they also play important roles in the brain, including regulation of neurogenesis, synaptic transmission, and behavior (Perez et al. 2015; Peters 2014). Within the brain, the hypothalamus has proven to be the main site of expression of imprinted genes, and from studies of knockout mouse models as well as human inherited disorders, it is evident that they influence neuroendocrine pathways, energy homeostasis, circadian rhythm, and social interactions (Ivanova and Kelsey 2011; Perez et al. 2015). In this chapter, we provide an overview of the hypothalamic functions of imprinted genes and highlight a few disease-relevant examples. In addition, we discuss techniques used in the identification and epigenetic analysis of imprinted genes and indicate currently open questions and trends in the field.

10.2. Main Features of Imprinted Gene Clusters

The importance of imprinting in mammals became evident from embryological studies, in which pro-nuclei of newly fertilized mouse eggs were transplanted in order to generate a genetically diploid bi-maternal (parthenogenetic) or a bi-paternal (androgenetic) conceptus. The embryos that developed from these concepti died in utero and showed growth aberration in embryonic and extraembryonic tissues (Ferguson-Smith 2011). These observations demonstrated that a diploid genome as such is not sufficient for normal mammalian development, that the two parental genomes make different functional contributions to embryonic development and that there must be some kind of "mark," which mediates the distinct functions of the maternal and paternal genomes, respectively. Thus, genomic imprinting became a paradigm that drove research into "epigenetic" mechanisms (Ferguson-Smith 2011). We know today that those epigenetic "marks" represent methylation of genomic DNA, histone modifications, and noncoding RNA expression.

In the majority of cases, imprinted genes are typically found in clusters of 3–12 genes spread over 20 Kb–3.7 Mb of DNA (Ferguson-Smith 2011; Peters, 2014) and they are usually regulated by the presence of DNA methylation on one parental allele in so-called Differentially Methylated Regions (DMRs). These regions are characterized by a high density of CpG dinucleotides (above 55%), termed CpG islands (CGIs). Here, methylation of cytosines occurs at the C5 position of the pyrimidine ring and is catalyzed by DNA methyltransferases (DNMTs) (Lyko 2018). A DMR is termed an Imprinting Control Region (ICR), if the differential methylation is established already in the germ cells and if functional studies have proven that it controls the imprinting of associated genes within a cluster. Thus, ICRs regulate gene expression and chromatin structure over long distances (Ferguson-Smith 2011). Maternally methylated DMRs and ICRs are usually located at promoters while paternally methylated DMRs and ICRs are located in intergenic regions (Bartolomei and Ferguson-Smith 2011).

DNA methylation is established during gametogenesis, resists the extensive genomic reprogramming that occurs after fertilization and is maintained in the offspring throughout life (Fig. 10.1). For inheritance of imprinted gene expression to the next generation, the primordial germ cells of an embryo undergo a phase of erasure of DNA methylation, followed by re-establishment of methylation at DMRs/ICRs according to the sex of the individual and mediated by DNMT3A and the accessory protein DNMT3L (Bartolomei and Ferguson-Smith 2011; Plasschaert and Bartolomei 2014). How the ICRs are recognized within the genome is still unknown, but it is clear that several factors are involved in the maintenance of DNA methylation, including *ZINC FINGER PROTEIN HOMOLOG 57* (*ZFP57*) and *Developmental pluripotency-associated 3* (*Dppa3*). Mutations in these genes result in loss of imprinting at several loci during early embryogenesis, which in turn causes a range of disease symptoms (Ferguson-Smith 2011; Plasschaert and Bartolomei 2014).

Before discussing techniques and methods used in the analysis of allelic expression and epigenetic regulation of imprinted genes, we first provide an overview about the functional roles of imprinted genes in the hypothalamus and, where applicable, their involvement in human neurodevelopmental disorders. Then, in the context of the Prader–Willi syndrome (PWS)/Angelman syndrome (AS) imprinting cluster and the *Gnas* locus, we discuss the structure and organization of regulatory elements of imprinted genes.

10.3. Functions of Imprinted Genes in the Hypothalamus

When the first imprinted genes (*Igf2*, *Igf2r,* and *H19*) were identified, they were found to affect mainly embryonic growth, placental function, and nutrient supply and demand at the maternal–fetal interface (Ferguson-Smith 2011; Peters 2014; Plasschaert and Bartolomei 2014). However, it soon became apparent that a number of imprinted genes were expressed in defined brain regions, and many of them showed high

expression levels specifically in the hypothalamus (Ivanova and Kelsey 2011). Phenotype analyses of knockout mouse models and clinical case studies of human imprinting disorders revealed that many imprinted genes continue to impact growth and whole-body energy homeostasis beyond embryonic development and into adulthood via influencing neuroendocrine pathways and the autonomic nervous system. Other core functions of the hypothalamus, including circadian rhythms, reproductive functions, and maternal-infant care behavior are also deregulated upon the deficiency of some imprinted genes. We will first describe the hypothalamic roles of the *Gnas* and the PWS-AS loci since they have been analyzed in some detail, before summarizing findings related to other imprinted genes.

10.3.1. Hypothalamic Regulation of Energy Homeostasis by *Gnas* and *Gnasxl*

The *Gnas* imprinted locus on mouse chromosome 2 and human chromosome 20 comprises a complex arrangement of protein-coding and noncoding transcripts, alternative promoters, and epigenetically controlled regulatory elements (Fig. 10.2a) (Chen et al. 2011; Peters 2014). The two protein-coding transcripts *Gnas* and *Gnasxl* derive from different first exons, but share exons 2–12. As the open reading frames are conserved, the two proteins Gαs and XLαs only differ at their NH_2-termini, thus forming alternative versions of the G-protein α-stimulatory subunit. Both can mediate signal transduction from seven transmembrane receptors to adenylate cyclase and cAMP formation, although XLαs can also stimulate the inositol 1,4,5-trisphosphate (IP3)/protein kinase C (PKC) second messenger pathway in some cell types (He et al. 2015). While *Gnasxl* is exclusively expressed from the paternal allele, *Gnas* is biallelically expressed in most tissues, but monoallelically transcribed from the maternal allele in specific cell types of the brain, renal proximal tubules, thyroid gland, pituitary somatotroph cells and the ovary (Chen et al. 2011). The third protein-coding transcript, maternal allele-derived *Nesp*, generates a neuroendocrine secretory protein (Nesp55) from an open reading frame that is confined to its upstream exon, although the RNA is spliced onto downstream exons 2–12 of *Gnas*. The regions of differential DNA methylation (ICRs at *Nespas-Gnasxl* and *exon-1a*; DMR at *Nesp*), the noncoding transcripts *Nespas* and *exon-1a*, as well as the *Nesp* transcript have a role in the establishment and regulation of genomic imprinting at the cluster (Plagge 2012). Both ICRs become methylated in the maternal germ cells, and the methylation on the maternal allele is maintained in somatic tissues of the offspring. The ICR at *Nespas-Gnasxl* controls the imprinting of all transcripts of the locus, while the ICR at *exon-1a* only regulates the monoallelic expression of *Gnas* in those specific tissues mentioned above. The DNA methylation on the maternal allele inhibits the transcription of *Gnasxl*, *Nespas,* and *exon-1a*. On the paternal allele, the unmethylated ICRs serve as promoters for the noncoding RNAs *Nespas* and *exon-1a*, which silence *in cis* the expression of *Nesp* and *Gnas* via unclear mechanisms that involve histone modifications (Mehta et al. 2015).

Fig. 10.2

Simplified schemes of the *Gnas* and the PWS-AS (*Snrpn-Ube3a*) imprinted loci. The features of the maternal and paternal alleles are indicated in red and blue, respectively. Genes or transcripts are ~~is~~ named in the central part. Arrows mark transcription start sites and undulating lines noncoding RNAs. Open and filled boxes represent noncoding and coding exons, respectively, while black boxes indicate silenced genes. Differentially methylated regions of DNA (DMRs) are marked by MMM. (**a**) For the *Gnas* locus, the alternatively spliced coding transcripts and proteins are named above and below the alleles. DMRs at *Nespas* and *Exon 1A* (*EXON A/B* in human) are established in the maternal germline, while methylation at *Nesp* occurs during early embryonic development. *Gnas* is expressed biallelically, but is silenced on the paternal allele in some tissues (hatched box). *Nesp* represents a coding transcript (ORF limited to *Nesp* exon 2). *Nespas* is expressed from the unmethylated imprinting control region (ICR) of the locus. (**b**) The PWS-AS-associated *Snrpn-Ube3a* imprinting cluster contains several genes (represented by

single-exon boxes) that show monoallelic expression in the brain. *Ube3a* is biallelically expressed in most tissues, but silenced on the paternal allele in neurons (hatched box). The *Snrpn* long noncoding RNA occurs in multiple, variably processed forms, including brain-specific variants that overlap with *Ube3a* (interrupted undulating lines). *Snord115* and *Snord116* represent clusters of C/D box snoRNAs, which are generated from the *Snrpn* transcript. The bipartite ICR of the human locus is indicated as AS-IC and PWS-IC, the latter being conserved in mouse around the main *Snrpn* start site. *NPAP1* is not present in the murine locus, but *Peg12* is imprinted in mice. Somatic DMRs at *Ndn* and *Mkrn3* are established during development

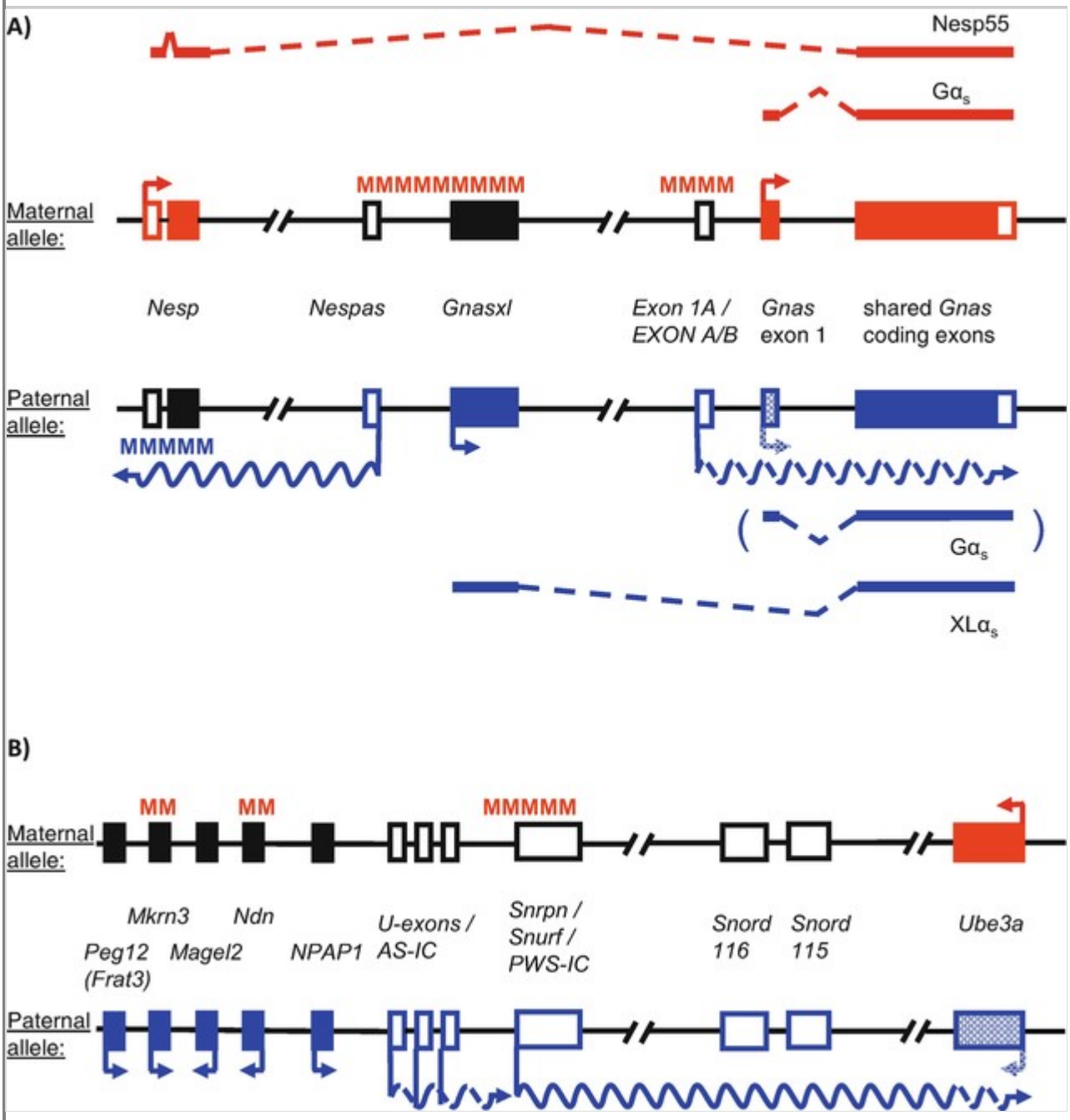

Hypothalamic functions have been shown for *Gnas* and *Gnasxl*, while behavioral phenotypes of *Nesp*

knockout mice could not be specifically attributed to a role in this brain region, although *Nesp* is expressed in the hypothalamus (Plagge et al. 2005). In humans, *GNAS* and *GNASXL* mutations or epigenetic deregulation cause complex neuroendocrine disorders termed Albright's Hereditary Osteodystrophy (AHO) and Pseudohypoparathyroidism (PHP), the symptoms of which are caused by hormone resistance in multiple tissues, including disruption of parathyroid hormone signaling in the kidney (Table 10.1) (Mantovani et al. 2018; Turan and Bastepe 2013). Hypothalamus-associated symptoms are related to postnatal growth, feeding, and regulation of energy balance at the adult stage. Homozygous mutations of *Gnas* in mice are embryonic lethal and heterozygous mutations show different phenotypes, dependent on whether they were maternally or paternally inherited, whereby the mouse phenotypes largely reproduce the human disease symptoms. Due to genomic imprinting, maternally inherited mutations in shared exons only affect the *Gnas* transcript, but in those tissues, in which it is imprinted, Gαs function will be completely lost, while a 50% reduction occurs in cells with biallelic expression. On the other hand, paternally inherited mutations in shared exons will result in loss of XLαs and a 50% reduction of Gαs in cells with biallelic expression.

Table 10.1

Functions of imprinted genes in the hypothalamus and related human disorders

AQ2

Gene	Protein/RNA function	Expressed allele	Hypothalamus-related mouse knockout phenotype	Human disorder
Gnas	G-protein α-stimulatory subunit (Gαs); (intracellular signaling)	*Biallelic in most tissues; maternal allele in specific cell types*: PVN, DMH, and subset of MC4R-expressing neurons in the brain, proximal renal tubules, thyroid gland, pituitary somatotroph cells, and ovary	*Maternally inherited mutation*: obesity, reduced energy expenditure, reduced SNS activity, impaired melanocortin receptor-mediated stimulation of energy expenditure and blood pressure, reduced blood pressure and heart rate, decreased locomotor activity, glucose intolerance, insulin resistance *Paternally inherited mutation*: normal energy homeostasis	Albright's Hereditary Osteodystrophy (AHO) and Pseudohypoparathyroidism (PHP) Hypothalamus-associated symptoms when *maternally inherited*: obesity, reduced SNS outflow Symptoms related to other tissues when *maternally inherited*: renal parathyroid hormone resistance, hypocalcemia, hyperphosphatemia, TSH resistance, GHRH resistance *Parent-of-origin independent symptoms*: short stature, brachydactyly, heterotopic ossifications, and other variable features
Gnasxl	Extra large G-protein α-stimulatory subunit (XLαs); (intracellular signaling)	Paternal	*Postnatally*: growth retardation, hypoglycemia, reduced milk intake, reduced lipid stores in adipose tissue *Adult stage*: decreased adiposity and body weight, elevated SNS activity, elevated metabolic rate and body temperature, increased blood pressure and heart rate, increased glucose tolerance, and insulin sensitivity	*Pre- and neonatal symptoms* Small for gestational age/intrauterine growth retardation, low birth weight, postnatal growth retardation, feeding problems, low body mass index during childhood

Gene	Protein/RNA function	Expressed allele	Hypothalamus-related mouse knockout phenotype	Human disorder
Magel2	MAGE family ubiquitin ligase regulator (endosomal protein sorting and recycling)	Paternal	*Postnatally*: 10–50% mortality; diminished oxytocin-induced suckling initiation after birth; reduced neonatal hypothalamic levels of oxytocin, arginine-vasopressin, and orexin-A *Adult stage*: increased fat mass despite reduced food intake and orexin-A levels, reduced lean mass; hypothalamic leptin resistance; reduced POMC neurons and projections; rhythmic circadian expression in SCN and altered/reduced circadian activity patterns; and abnormal behavior	Prader–Willi syndrome
Ndn (Necdin)	MAGE family ubiquitin ligase regulator	Paternal	High rate of early neonatal mortality due to respiratory deficiencies (brainstem related); fewer hypothalamic oxytocin and gonadotropin-releasing hormone neurons; reduced thyrotropin-releasing hormone levels in PVN and hypothyroidism; abnormal axon bundles; and behavioral abnormalities	Prader–Willi syndrome
Snord116	Box C/D small nucleolar RNA	Paternal	Postnatal and adult growth retardation; reduced adiposity; increased energy expenditure; resistance to high-fat diet-induced obesity; improved body temperature maintenance at 4 °C; behavioral abnormalities Adult-onset deletion in mediobasal hypothalamus: hyperphagia and obesity	Prader–Willi syndrome
Ube3a	Ubiquitin-protein ligase E3A; (protein degradation)	Biallelic in most tissues; maternal allele in brain	Sleep disturbances, circadian rhythm regulation via *Bmal1*	Angelman syndrome
Dlk1	Protein delta homolog 1, (Trans-membrane and	Paternal	Hypothalamus-related functions uncertain, potentially involving postnatal growth	Central precocious puberty; increased fat mass (Temple syndrome)

Gene	Protein/RNA function	Expressed allele	Hypothalamus-related mouse knockout phenotype	Human disorder
	secreted protein with similarity to Notch ligands)		retardation	
Dio3	Thyroxine 5-deiodinase (thyroid hormone catabolism)	Paternal (e.g., neonatal hypothalamus, tissue- and stage-specific)	Postnatal and adult growth retardation; reduced adiposity; abnormal thyroid hormone regulation and hypothalamus–pituitary–thyroid axis; increased energy expenditure and locomotion; changes in hypothalamic gene expression of leptin-melanocortin, oxytocin, and vasopressin pathways; abnormal circadian activity; impaired viability and fertility	Potentially involved in Temple syndrome
Kcnq1	Potassium voltage-gated channel subfamily KQT member 1	Maternal	No hypothalamus-related phenotype described, but range of other symptoms	Growth hormone deficiency and gingival fibromatosis, QT syndrome, auditory and cardiac symptoms
Peg3	Zinc finger DNA-binding protein	Paternal	Reduced body weight throughout life; increased adiposity; leptin resistance; reduced metabolic rate; lower body temperature; altered hypothalamic neuropeptide expression	

Gnas and *Gnasxl* transcript- and tissue-specific knockout mouse models have shed some light onto the functions of the two proteins in the hypothalamus and revealed opposite or antagonistic impacts of Gαs and XLαs on energy balance and sympathetic nervous system (SNS) activity (Weinstein 2014). Conditional gene targeting of the *Gnas*-specific exon 1 and its brain-specific deletion (via Nestin-Cre strain) on the maternally inherited chromosome causes severe obesity due to decreased energy expenditure and O_2 consumption, lower locomotor activity, reduced SNS outflow, body temperature, and heart rate (Table 10.1). Glucose intolerance and insulin resistance were also observed. These symptoms are, however, not found in the paternally inherited, brain-specific knockout, which show normal energy homeostasis. These findings indicate genomic imprinting in the brain. The response to stimulation of the melanocortin receptors (MC3R, MC4R), which mediate the anorexigenic response downstream of leptin signaling, was found to be blunted in these mice. However, the maternally inherited *Gnas* mutation specifically disrupts the energy expenditure-stimulating functions of melanocortins, while their food intake-reducing effects remained intact (Chen et al. 2009). The mechanism(s) underlying these responses are unclear. The decreased energy expenditure in the mutants has been linked to reduced SNS outflow as levels of norepinephrine and uncoupling protein 1 (UCP1) in brown adipose tissue (BAT), as well as heart rate and blood pressure are

reduced.

Monoallelic maternal expression of *Gnas* is found in the paraventricular nucleus (PVN) of the hypothalamus (Chen et al. 2009). A specific maternal allele knockout of *Gnas* in the PVN, using a Sim1-Cre strain, reproduced a much milder obesity phenotype than observed with the Nestin-Cre line described above suggesting that imprinted Gαs expression in additional brain regions contributes to the earlier observed phenotype (Chen et al. 2012). However, it does reproduce the lower blood pressure and heart rate of the whole-brain knockout. Maternal allele-specific Gαs is also required in the PVN to mediate melanocortin-induced blood pressure increases (Li et al. 2016). In contrast to the brain knockout, the SNS stimulation of BAT, cold-induced thermoregulation as well as the melanocortin induction of energy expenditure are intact in the PVN-specific *Gnas* knockout, indicating that these physiological responses are mediated by other neurons (Chen et al. 2012). Further investigations by the group of L. S. Weinstein excluded the ventromedial hypothalamus (VMH) and identified the dorsomedial hypothalamus (DMH) as a major site of imprinted Gαs regulation of energy expenditure (Chen et al. 2017). Adenovirus-mediated Cre-deletion of *Gnas* on the maternal allele in the DMH resulted in a number of changes including obesity, reduced energy expenditure, heart rate, and locomotor activity, as well as a blunted response to melanocortin-induced O_2 consumption. Baseline activation of BAT was reduced as seen in whole-brain knockout mice, but cold-induced activation of BAT and maintenance of body temperature were intact, as was food intake (Chen et al. 2017). Blood pressure was normal in the DMH-specific deletion of Gαs, in line with previous findings attributing this *Gnas* function to the PVN. However, when *Gnas* was deleted on the maternal allele in the DMH, stimulation of MC3/4R in the DMH did not lead to phosphorylation of cAMP response element-binding protein (CREB) (Chen et al. 2017). These findings are consistent with maternal allele-specific expression of Gαs in the DMH, which is required for basic and melanocortin-induced stimulation of energy expenditure.

Recently, the importance of *Gnas* for mediating the melanocortin effects on energy homeostasis was confirmed through a specific knockout in MC4R-expressing neurons (Podyma et al. 2018). Homozygous deletion of *Gnas* in MC4R neurons results in severe obesity, while maternal allele-specific deficiency leads to a milder phenotype. Paternal heterozygous knockouts showed normal energy balance. Reduced energy expenditure and locomotor activity also featured in homozygous *Gnas* MC4R-specific knockouts, but the major contributor to the obesity in these mice was increased food intake, which was not observed in the other maternal allele-specific hypothalamus knockouts described above (Podyma et al. 2018). The milder obesity in mice with maternal allele-specific disruption of *Gnas* in MC4R neurons was attributable to reduced energy expenditure with food intake being unchanged. Furthermore, while homozygous knockouts could not maintain body temperature in a cold environment, heterozygous maternal knockouts of *Gnas* in MC4R neurons showed thermoregulation in line with previous observations in PVN- and DMH-specific deletions (Chen et al. 2012, 2017; Podyma et al. 2018).

In summary, stimulation of SNS outflow appears to be at the heart of the metabolic functions regulated by ~~$G\alpha_s$~~ Gαs expression from the maternal allele. But it is also apparent that *Gnas* expression from the maternal allele regulates various branches of the SNS, affecting cardiovascular phenotypes via the PVN and energy expenditure via the DMH, which projects to the raphe pallidus of the medulla and other SNS-relevant brain areas. Its pathway of regulating cold-induced thermogenesis, however, remains as yet unknown (Chen et al. 2012, 2017; Podyma et al. 2018). Although disruption of MC3/4R signaling contributes substantially to the energy homeostasis phenotypes of central nervous system-specific *Gnas* knockouts, it is currently unclear whether Gαs signaling from other receptors might also contribute.

In contrast to *Gnas*, the *Gnasxl* knockout mouse phenotype, as well as case reports in human, indicate that the extra-large variant XLαs has overtly antagonistic functions to Gαs in the regulation of energy homeostasis and SNS activity (Weinstein 2014). *Gnasxl* is expressed in all major hypothalamic areas (apart

from the VMH), the suprachiasmatic nucleus (SCN), preoptic area, and SNS-associated nuclei in the medulla, e.g., the raphe pallidus, nucleus of the solitary tract, as well as the intermediolateral layer of the spinal cord (Krechowec et al. 2012; Plagge et al. 2004). Expression of *Gnasxl* in peripheral tissues, for example, muscle tissues, becomes silenced postnatally with only a few exemptions like the adrenal medulla (Krechowec et al. 2012; Xie et al. 2006). Newborn XLαs-deficient pups become growth retarded, take in less milk and display hypoglycemia and lack of lipid reserves in adipose tissue, all of which results in a high mortality rate in the first week (Table 10.1; Plagge et al. 2004; Xie et al. 2006). Those *Gnasxl* knockout mice that survive to weaning age, develop into fertile adults, but remain underweight and lean throughout life, despite relatively increased food intake. Furthermore, their phenotype consists of increased energy expenditure, metabolic rate, body temperature, blood pressure, and heart rate, which is associated with elevated SNS outflow (Nunn et al. 2013; Xie et al. 2006). They also show improved glucose tolerance and insulin sensitivity (Xie et al. 2006). The precise neural pathways through which *Gnasxl* regulates SNS outflow and energy homeostasis remain unresolved, as are the neural receptors that signal via XLαs.

Human disease symptoms related to loss of *GNASXL* function have been difficult to ascertain since mutations that specifically disables the first *GNASXL* exon have not been identified. However, paternal transmission of mutations in shared downstream exons 2–13 and maternal uniparental disomies that encompass the *GNAS* locus on chromosome 20, which result in two maternal alleles and lack of a paternally inherited allele, indicate pre-/neonatal symptoms (Table 10.1). These include intrauterine growth retardation, low birth weight, postnatal growth retardation, and feeding problems (Genevieve et al. 2005; Kawashima et al. 2018; Mulchandani et al. 2016; Richard et al. 2013). Although no adult metabolic data of such patients have been reported, the neonatal symptoms are reminiscent of the *Gnasxl* knockout mouse phenotype (Plagge et al. 2004). Taken together, these findings show that XLαs exerts an important role in neonatal physiology in addition to its regulation of adult energy homeostasis, which to date has only been confirmed in mice.

In adults, XLαs acts in the brain to inhibit SNS outflow and energy expenditure, while its variant Gαs functions to stimulate SNS activity and metabolic rate. These antagonistic roles are correlated on the epigenetic level with genomic imprinting and monoallelic transcription from opposite parental alleles. *Gnasxl* is expressed exclusively from the paternal allele, while *Gnas* is only imprinted in specific hypothalamic neurons, where it is transcribed from the maternal allele. Why epigenetic regulation through genomic imprinting of crucial growth and energy homeostasis functions evolved in mammals is beyond the scope of this chapter, but has been extensively discussed in the literature (Haig 2004; Peters 2014).

10.3.2. Hypothalamic Functions of the Prader–Willi Syndrome (PWS) and Angelman Syndrome (AS) Imprinting Cluster

Another example of a cluster of imprinted genes with functions in the hypothalamus is the Prader–Willi syndrome and Angelman syndrome locus on human chromosome 15 (conserved on mouse chromosome 7) (Buiting et al. 2016; Cassidy et al. 2012; Peters 2014). The locus comprises five genes with paternal allele-specific expression (*MKRN3, MAGEL2, NDN, NPAP1*, and *SNURF/SNRPN/SNORD115-116*), and one with maternal allele-specific transcription (*UBE3A*), although the murine locus contains paternally expressed *Peg12* instead of *NPAP1* (Fig. 10.2b). Loss of function of the paternally expressed genes causes PWS, while loss of function of the maternally expressed *UBE3A*, which is imprinted in the brain only, causes AS. The monoallelic expression of all genes in the cluster is controlled by a bipartite ICR that encompasses the promoter of the *Snurf/Snrpn/Snord115–116* gene (PWS-IC) and additional sequences further upstream (AS-IC). The PWS-IC is methylated on the maternal allele, thus silencing the expression of the long *Snurf/Snrpn /Snord115–116* RNA. In neurons, this paternally expressed transcript, which is also known as *Ube3a antisense* and can be processed in different ways, extends into *Ube3a* exons and is thought to inhibit the

expression of *Ube3a* in *cis* through transcriptional interference, thus resulting in intact *Ube3a* expression only from the maternal allele (Buiting et al. 2016; LaSalle et al. 2015). On the paternal allele, the PWS-IC remains unmethylated and has an activation function for all other paternally expressed genes of the cluster, which involves physical interactions via chromosome looping (Plagge 2012).

AQ3

Angelman syndrome constitutes a neurodevelopmental disorder that is mainly characterized by intellectual disability, microcephaly, speech impairment, happy demeanor, EEG abnormalities and sleep disturbances (Buiting et al. 2016). Functionally, Ube3a (Ubiquitin-protein ligase 3a) is involved in labeling proteins for degradation and lack of the enzyme impairs synapse formation and remodeling. Little is known about hypothalamus-specific roles of Ube3a in the context of AS, but knockout mice show abnormalities in sleep and circadian rhythm, potentially due to impaired Ube3a-mediated degradation of the circadian clock protein Bmal1 in the hypothalamus (Ehlen et al. 2015; Shi et al. 2015). On the other hand, main symptoms of PWS are postnatal hypotonia, poor suckling, failure to thrive, respiratory disturbances, hypogonadism, childhood-onset obesity, hyperphagia, cognitive and behavioral abnormalities, short stature, and growth hormone insufficiency (Cassidy et al. 2012). Knockout mouse models indicate that all paternally expressed genes contribute to the range of these symptoms.

The functions of *Magel2* (*Mage-like protein 2*) have been characterized, and it is highly expressed in many areas of the hypothalamus (Tacer and Potts 2017). On a molecular level, Magel2 acts as a regulator of RING E3 ubiquitin ligases within a complex that controls endosomal protein sorting. Deficiency of Magel2 in a hypothalamic cell line impairs protein recycling to the plasma membrane (Tacer and Potts 2017). The physiological functions of *Magel2* are indicated by knockout mice, which show 10–50% pre-weaning mortality (Table 10.1) (Kozlov et al. 2007; Schaller et al. 2010). This mortality occurs in the first few hours after birth, due to a deficiency in oxytocin in the pups, which at this stage is required to initiate suckling activity (Schaller et al. 2010). For surviving knockout mice, a slight postnatal growth retardation is followed at the adult stage by reduced lean mass, increased fat mass despite decreased food intake and hypothalamic orexin-A (Bischof et al. 2007; Kozlov et al. 2007). It is noteworthy that the observation of reduced food intake is contrary to PWS symptoms. Hypothalamic POMC neurons and their projections were found to be deficient in knockout mice (Maillard et al. 2016; Mercer et al. 2013), and leptin resistance might be related to reduced leptin receptor recycling from endosomes to the plasma membrane (Wijesuriya et al. 2017). The Magel2 protein is also robustly expressed in the SCN and its levels fluctuate with circadian rhythmicity (Kozlov et al. 2007). Consistent with SCN function, the knockout mice show overall reduced wheel-running activity and disturbed activity patterns under constant darkness (Kozlov et al. 2007; Tacer and Potts 2017).

Similar to *Magel2*, *Necdin* (*Ndn*) constitutes another member of the Mage family of proteins (Tacer and Potts 2017). *Necdin* is expressed in a number of brain regions, and it has roles in neuronal survival, migration, differentiation, and neurite formation (Table 10.1). *Ndn* knockout mice have neonatal respiratory problems, which lead to a substantial rate of mortality shortly after birth (Gerard et al. 1999; Muscatelli et al. 2000). Respiratory disturbances are also observed in PWS and they are due to defects in the serotoninergic system of the brainstem inspiratory rhythm generator (Matarazzo et al. 2017). In the hypothalamus, lack of *Ndn* causes reduced numbers of oxytocinergic neurons in the PVN and gonadotropin-releasing hormone neurons in the preoptic area (Miller et al. 2009; Muscatelli et al. 2000). Deficits in the latter neuron population might be responsible for the hypogonadism observed in PWS. *Necdin* knockout mice present symptoms of hypothyroidism due to reduced levels of thyrotropin-releasing hormone in the PVN (Hasegawa et al. 2012). Furthermore, Necdin has a role in axon outgrowth as indicated by aberrant axon bundles in the anterior hypothalamus and other brain regions (Lee et al. 2005). On the molecular level, Necdin appears to interact with a diverse set of binding partners, including cytoskeleton-associated proteins as well as transcription factors (Hasegawa et al. 2012; Lee et al. 2005).

The box C/D small nucleolar RNA cluster *Snord116* also has a crucial role in PWS (Cavaille 2017). Patients with microdeletions of this cluster, but intact *NECDIN* and *MAGEL2* genes, present with PWS symptoms, and knockout mouse models also show some of these disease characteristics (Bieth et al. 2015; Ding et al. 2008; Skryabin et al. 2007). Postnatal growth retardation is a shared feature in humans and mice with paternally inherited *Snord116* deletions. However, knockout mice remain lean and underweight throughout life due to increased energy expenditure, while *SNORD116*-mutant patients develop the typical PWS hyperphagic obesity toward adulthood (Bieth et al. 2015; Ding et al. 2008; Skryabin et al. 2007). Interestingly, when the *Snord116* cluster is deleted in the mediobasal hypothalamus of adult mice via an adenovirus Cre-recombinase vector injection, the mutant mice then develop hyperphagia and obesity reminiscent of PWS patients (Polex-Wolf et al. 2018). These findings highlight physiological differences between humans and mice and potentially indicate species-specific compensatory abilities to inherited gene mutations during development.

10.3.3. Other Imprinted Genes with Hypothalamic Functions

Although less well characterized, four other imprinted genes have roles in the hypothalamus, which are briefly summarized here. A cluster of imprinted genes on mouse chromosome 12 (human chromosome 14) contains two protein-coding genes with hypothalamic functions, *Dlk1* (*Protein delta homolog 1*) and *Dio3* (*Thyroxine 5-deiodinase*), both expressed from the paternal allele (Table 10.1). The Dlk1 protein has structural similarity to Notch ligands, but its precise signaling mechanism is unknown. Dlk1 is prominently expressed in several hypothalamic nuclei (arcuate nucleus, PVN, DMH, and SCN), and it has been co-localized in oxytocin, arginine–vasopressin, orexin, NPY, and dynorphin-positive neurons (Meister et al. 2013; Villanueva et al. 2012). *Dlk1* involvement in embryonic development and adiposity has been well characterized, but its hypothalamus-specific functions are poorly understood. A mutation of *DLK1* in humans leads to central precocious puberty, possibly via GnRH-neuron regulation, and increased fat mass (Dauber et al. 2017). *Dio3* shows monoallelic expression from the paternal allele in the neonatal hypothalamus (Martinez et al. 2014). Knockout mice display postnatal growth retardation, which lasts into adulthood, deregulated thyroid hormone levels and disturbances in the hypothalamic–pituitary–thyroid axis (Table 10.1). Reduced adiposity is associated with changes in hypothalamic gene expression of the leptin–melanocortin pathway, increased energy expenditure, and locomotion (Wu et al. 2017). Activity patterns of knockout mice also showed circadian changes, which might be associated with *Dio3* expression in the SCN. Additional behavioral abnormalities relating to aggression and maternal care of the knockout mice are associated with changes in the hypothalamic oxytocin and arginine–vasopressin systems (Stohn et al. 2018). The third gene is the voltage-gated potassium channel gene *Kcnq1*, which is located in a large imprinting cluster on mouse chromosome 7 (human chromosome 11) and is expressed from the maternal allele. It has a crucial role in the hypothalamic–pituitary growth hormone axis. The potassium channel is expressed in hypothalamic growth hormone-releasing hormone (GHRH) neurons and pituitary somatotropes. *KCNQ1* mutations in humans cause growth hormone deficiency and gingival fibromatosis among other symptoms (Table 10.1) (Tommiska et al. 2017). The fourth imprinted gene associated with hypothalamic functions is the *Paternally expressed gene 3* (*Peg3*), a Zinc finger-containing DNA-binding factor that is widely expressed in the hypothalamus (Li et al. 1999). *Peg3* knockout mice have reduced body weight at all stages of life, but are hypometabolic, show a proportionately increased fat mass, lower body temperature, leptin resistance and changes in hypothalamic NPY, POMC, MCH, and Orexin neuropeptide expression (Curley et al. 2005). Whether knockout females show deficiencies in maternal behavior toward their offspring (e.g., nest building, pup retrieval, nursing) that are linked to a reduced number of hypothalamic oxytocin neurons, is controversial (Li et al. 1999; Denizot et al. 2016).

10.4. Analysis of Genomic Imprinting

10.4.1. Analysis of Methylation

As mentioned in the introduction, the canonical regulatory mechanism of imprinting is the methylation of DNA at specific CGIs to form DMRs or ICRs. A breakthrough in the study of DNA methylation was achieved with the technique of bisulfite conversion of genomic DNA. The treatment with sodium bisulfite promotes the deamination of cytosine residues, which is followed by desulfonation at elevated pH, thus leading to conversion into uracil (Fig. 10.3). When a residue is methylated, however, the deamination cannot take place and the cytosine remains unchanged. Since only cytosines in single-stranded DNA are susceptible to conversion by bisulfite, complete DNA denaturation is a critical step. After bisulfite conversion, the DNA fragment of interest can be amplified by PCR using primers designed to anneal to either the sense or the antisense DNA strand, which at this point are not complementary anymore. The PCR primer design needs to be based on the expected bisulfite-converted sequence, in which methylated cytosines will be retained as C, and the unmethylated cytosines converted to uracil, i.e., such primers are usually AT-rich (Fig. 10.3). Furthermore, AT-rich bisulfite PCR amplicons (from originally unmethylated DNA) can be difficult to amplify using standard Taq-Polymerases and, therefore, amplicon sizes of less than ~400 bp are recommended. Small amplicon size is especially important when allelic differences in methylation are investigated to avoid a bias in amplification of originally methylated over unmethylated alleles, i.e., to minimize preferential amplification of templates with more balanced nucleotide composition over highly AT-rich templates. The advantages of the bisulfite method include the efficiency of the chemical conversion, relatively low cost and the speed of the procedure. Because in one reaction the whole genome can be converted and investigated in subsequent analyses, this has become the best approach for the study of DNA methylation.

Fig. 10.3

Bisulfite conversion of genomic DNA. The treatment with $NaHSO_3$ induces the deamination of cytosine into uracil residues. This conversion will not happen, if the cytosine is methylated or hydroxy-methylated in the carbon 5 position. Following bisulfite treatment, the sense and antisense strands of the original double-stranded DNA are no longer complementary. PCR amplification of a strand will now lead to an exchange of uracil residues to thymine and the DNA sequence will then be characterized by an abundance of A and T. Only the methylated sites will retain cytosine residues. The primers for bisulfite sequencing need to be complementary to the converted sequence (orange and green arrows). Black lollipops indicate methylated CpG sites

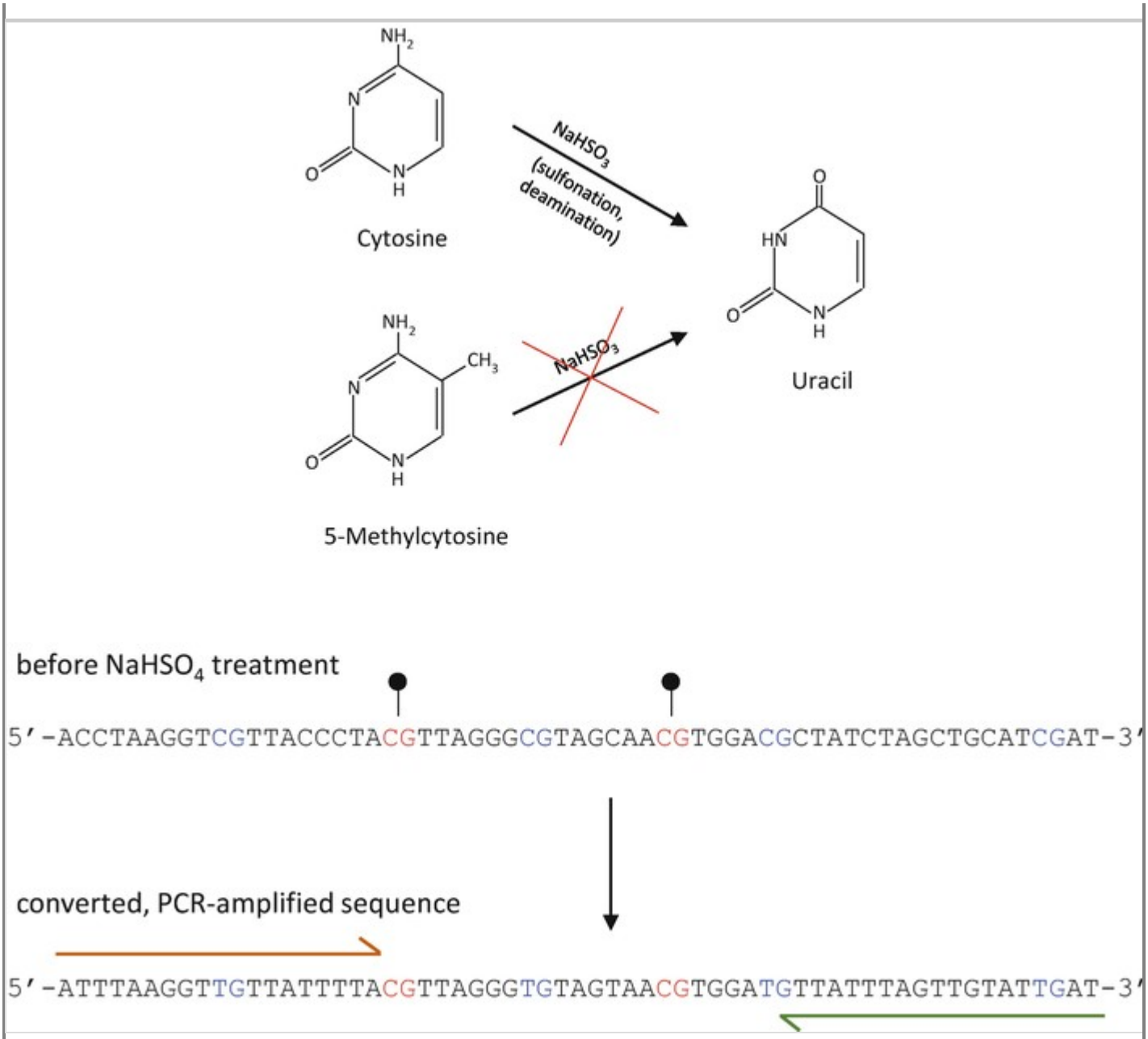

Following bisulfite conversion and PCR amplification, the DNA fragment of interest can be further analyzed using several methods. Traditionally, the PCR product can be cloned into a plasmid and then a sufficiently large number of individual clones sequenced via Sanger sequencing. This procedure will produce a representation of the frequency of methylated (preserved) and unmethylated (converted) cytosines at every CpG dinucleotide position of the DNA amplicon in the cloned population (Fig. 10.4a). In the analysis of a DMR of an imprinted gene, a ratio of ~50% methylation would be expected at each CpG site whereby two types of sequences should be distinguishable: predominantly methylated and predominantly converted (Fig. 10.4a). If the DNA fragment of interest was isolated from hybrid offspring of different mouse strains and contains a single nucleotide polymorphism (SNP), the methylation can be associated with the parental origin of the allele.

Fig. 10.4

Analysis methods of bisulfite-treated and PCR-amplified genomic DNA. (**a**) Cloning and Sanger sequencing

of bisulfite PCR products. Scheme showing three examples of possible outcomes for methylation patterns in an amplicon covering a CGI. Each row of dots represents one cloned PCR product and each dot represents an individual CpG site (black = methylated, white = unmethylated). The differentially methylated example, which contains methylated and unmethylated sequences, would be typical of an imprinted DMR. Further SNP analysis would be required to associate the methylation status with the parental origin of an allele. (**b**) Combined bisulfite restriction analysis (COBRA) on untreated and bisulfite-treated genomic DNA from hippocampus, cerebral cortex, and kidney. Restriction enzyme BstUI recognizes the site CGCG. When a cytosine is unmethylated in the genomic DNA, it is converted to thymine following bisulfite treatment and PCR amplification, disrupting the integrity of the restriction sites. In contrast, methylated sequences maintain the cytosine and the restriction enzyme will cut the PCR amplicon. This example CpG island shows the presence of both methylated and unmethylated alleles (unpublished data). (**c**) Bisulfite pyrosequencing analysis of the same CGI as in (**b**). A pyrogram sequencing trace of a bisulfite PCR amplicon is shown. The positions highlighted in light blue represent CpG sites and the degree of methylation at each site is quantified and displayed as a percentage above the highlighted peaks (unpublished data)

AQ4

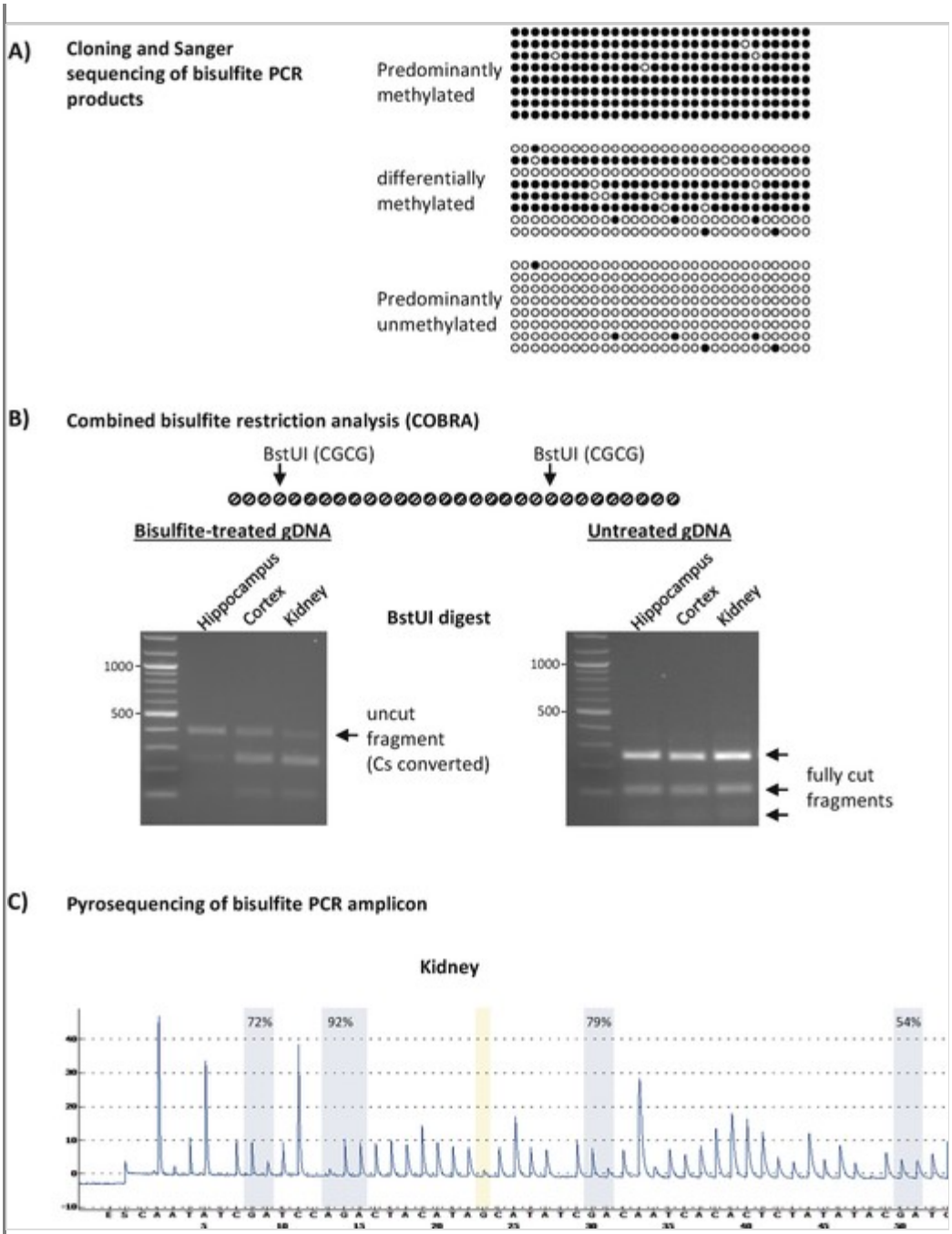

An alternative to cloning and sequencing consists of the digestion of a PCR product with restriction endonucleases that contain CpGs in their recognition sites such as TaqI (T/CGA) and BstUI (CG/CG) (Fig. 10.4b). This technique, called COBRA (combined bisulfite restriction analysis) (Eads and Laird 2002), detects originally methylated CpGs as they are conserved after bisulfite treatment and PCR amplification and then cut by the restriction endonuclease. By contrast, bisulfite conversion of an unmethylated CpG leads to loss of the restriction site. If a CpG is fully methylated, the PCR product will be completely digested, and vice versa (Fig. 10.4b). Quantification of partially methylated sites will require blotting of the gel, hybridization, and signal detection with a probe.

The presence of both cytosine and thymine in the same position following bisulfite treatment and PCR amplification can indicate partial methylation or potentially incomplete bisulfite conversion. In the bisulfite

sequencing approach, incomplete conversion can be recognized through the presence of remaining C residues outside of CpG dinucleotides—all of these should have been converted. A potential drawback of bisulfite sequencing is related to cloning biases that can occur in bacterial strains used for plasmid transformation after ligation of bisulfite PCR amplicons. In genomic imprinting, a DMR will result in bisulfite amplicons with different sequences derived from methylated and unmethylated alleles, respectively, and it is possible that the ligated amplicons are not equally propagated after transformation into *E. coli*, thus giving a wrong representation of methylation frequencies. On the other hand, in the COBRA method appropriate positive controls for restriction endonuclease functionality need to be included. For this reason, it is always recommended to confirm any results using at least two independent approaches.

The best approach to accurately quantify the methylation status is the use of pyrosequencing of bisulfite-converted genomic DNA (Dejeux et al. 2009). This method also includes PCR amplification as a first step after bisulfite treatment to generate fragments of ~100 bp. These are then sequenced by adding one nucleotide at a time and quantifying its incorporation through a cascade of enzymatic reactions that result in strictly proportional luciferase-mediated light emission. For example, at a partially methylated CpG site, incorporation of dGTP (originally methylated C) and dATP(αS) (originally unmethylated C) are tested consecutively, and the ratio of light emitted at the two nucleotide steps represents the percentage of methylated cytosine (Fig. 10.4c). Pyrosequencing is now accepted as the “gold standard” for quantitative sequencing. Apart from analyzing methylation at specific loci, bisulfite treatment has now been combined with next-generation sequencing to investigate the whole genome in specific tissues or cell types, for example, via whole-genome bisulfite sequencing (WGBS) (Harris et al. 2010). As details of the various approaches and the importance of avoiding biases at specific steps in the protocols cannot be covered here, we refer the reader to more specific, recently published work (Harris et al. 2010; Olova et al. 2018).

10.4.2. Analysis of Monoallelic Expression and Single-Cell Resolution of Imprinting

The analysis of imprinted genes also requires a proof of preferential or completely monoallelic gene expression in a parent-of-origin-specific way. To demonstrate this, exonic SNPs between different mouse strains are used, most commonly between C57BL/6J and *Mus musculus molossinus* (JF1) or *Mus musculus castaneus* (Cast/EiJ) strains. Tissues or cells from hybrid offspring of reciprocal parental crosses (e.g., C57BL/6J × JF1 and JF1 × C57BL/6J) are isolated, cDNA generated and the ratio of expression of the SNPs within the gene of interest determined via pyrosequencing. In the example shown in Fig. 10.5, expression of the *Trappc9* gene was found to be predominantly from the maternal allele (~70%) in brain tissue, while in kidney both SNPs show equal biallelic expression levels.

Fig. 10.5

SNP pyrosequencing to quantify allele-specific expression levels of a gene. Brain and kidney cDNAs were prepared from reciprocal crosses of C57BL/6J (B6) and Japanese fancy mouse 1 (*Mus musculus molossinus*, JF1), and a~~n~~ SNP-containing amplicon analyzed via pyrosequencing. Quantification of SNP prevalence indicates ~70% preferential maternal allele-specific expression of *Trappc9* in the brain, but equal biallelic expression in kidney. The reciprocal mouse crosses are shown as JF1/B6 and B6/JF1, whereby the first position conventionally indicates the maternal genotype. The SNP position is shaded in light blue

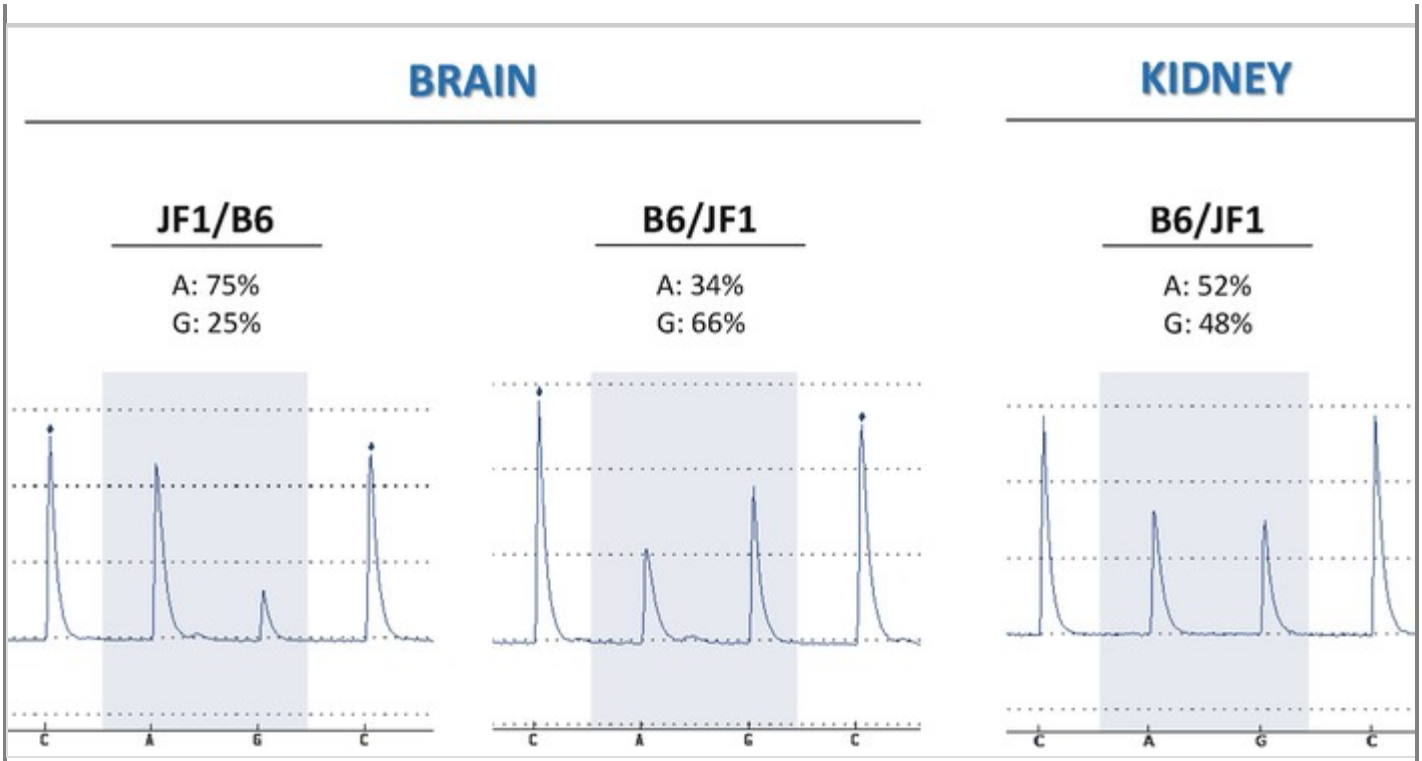

Recently, parent-of-origin biases of gene expression in the hybrid mouse brain have been characterized using RNAseq whole-transcriptome methods. In some cases, specific brain subregions, including the hypothalamus and arcuate nucleus were analyzed (Babak et al. 2015; Bonthuis et al. 2015; Huang et al. 2017; Perez et al. 2015). These transcriptome datasets, which include previously unknown transcripts, can be a good starting point for the investigation of imprinted genes in the brain. While several genes, including *Gnas*, *Dlk1,* and *Trappc9*, show tissue- or cell type-specific imprinting (Chen et al. 2009; Ferron et al. 2011; Perez et al. 2015), it is often unclear whether every cell within a population exhibits the parent-of-origin-specific, monoallelic expression. In particular, for genes with a bias toward parental allele-specific expression (e.g., 70% maternal, 30% paternal transcripts, based on whole tissue lysates) it remains unexplained whether such a ratio reflects unequal biallelic expression within each cell, or whether it is due to a mixture of cells with absolute monoallelic expression and cells with equal biallelic expression. This question is now being addressed with single-cell technologies. There are two main approaches to the single-cell analysis of allelic gene expression. On the one hand, probe hybridization onto fixed cells or tissue sections is combined with microscopy to distinguish between mono- or biallelic expression ~~in situ~~*in situ* (Bonthuis et al. 2015; Ginart et al. 2016; Huang et al. 2017). On the other hand, molecular genetics or genome-wide next-generation sequencing methods are applied on isolated single cell extracts (Angermueller et al. 2016; Cheow et al. 2015; Clark et al. 2018; Deng et al. 2014; Kelsey et al. 2017). As some of these techniques have been applied to hypothalamic tissues, we briefly describe them here as promising approaches for future research.

One of the methods designed to investigate allele-specific expression at the tissue level is “single nucleotide polymorphism RNA fluorescent in situ hybridization” (SNP-FISH) (Ginart et al. 2016; Levesque et al. 2013). The method is applied on tissues or cells from hybrid mice (e.g., C57BL/6J × Cast/EiJ), which harbor several SNPs in the mRNA of the gene of interest. Three different pools of fluorescently labeled oligonucleotides are then hybridized simultaneously to fixed samples: (a) a pool of “guide” probes, which bind to the mRNA of the gene of interest outside of the SNP regions for general detection of the relevant transcript; (b) two pools of SNP-specific oligonucleotides with different fluorescent labels, which vary only in a single nucleotide position to detect the parental origin of the transcript (Fig. 10.6). These SNP-specific oligos are initially

blocked by shorter “mask” oligonucleotides, leaving the SNP-containing region free to hybridize to the perfectly matching mRNA. Eventually, the SNP-specific oligos shed their “mask” oligos to fully anneal to the mRNA of interest. By analyzing co-localization of fluorescent signals from the “guide” oligos and the SNP-specific oligos, respectively, Ginart and colleagues (Ginart et al. 2016) were able to demonstrate that, within one tissue, cell populations with monoallelic maternal expression of the imprinted gene *H19* coexisted with neighboring cell populations that showed biallelic expression.

Fig. 10.6

Schematic illustration of the SNP-FISH technique for the detection of allele-specific RNA expression in cells and tissue sections. The allelic RNA variants of a gene of interest are shown with a~~n~~ SNP highlighted in red. A pool of fluorescently labeled “guide” oligonucleotides, which hybridize to non-variant sequences of the RNA, serve as a general marker for the presence of the transcript. Allele-specific oligonucleotides covering SNP positions (SNV probes) are labeled with a second and third fluorescent tag, respectively. Initially, only a short stretch of the SNV probe sequence (including the actual SNP position) is free to hybridize with the target RNA, as the remainder of the oligo is bound by a short complementary “mask” oligo. This allows specific binding of the SNV probes to the allelic RNA variants. The “mask” oligos are then displaced as the allele-specific oligos fully anneal with their target RNAs. Figure adapted from Levesque et al. (2013)

AQ5

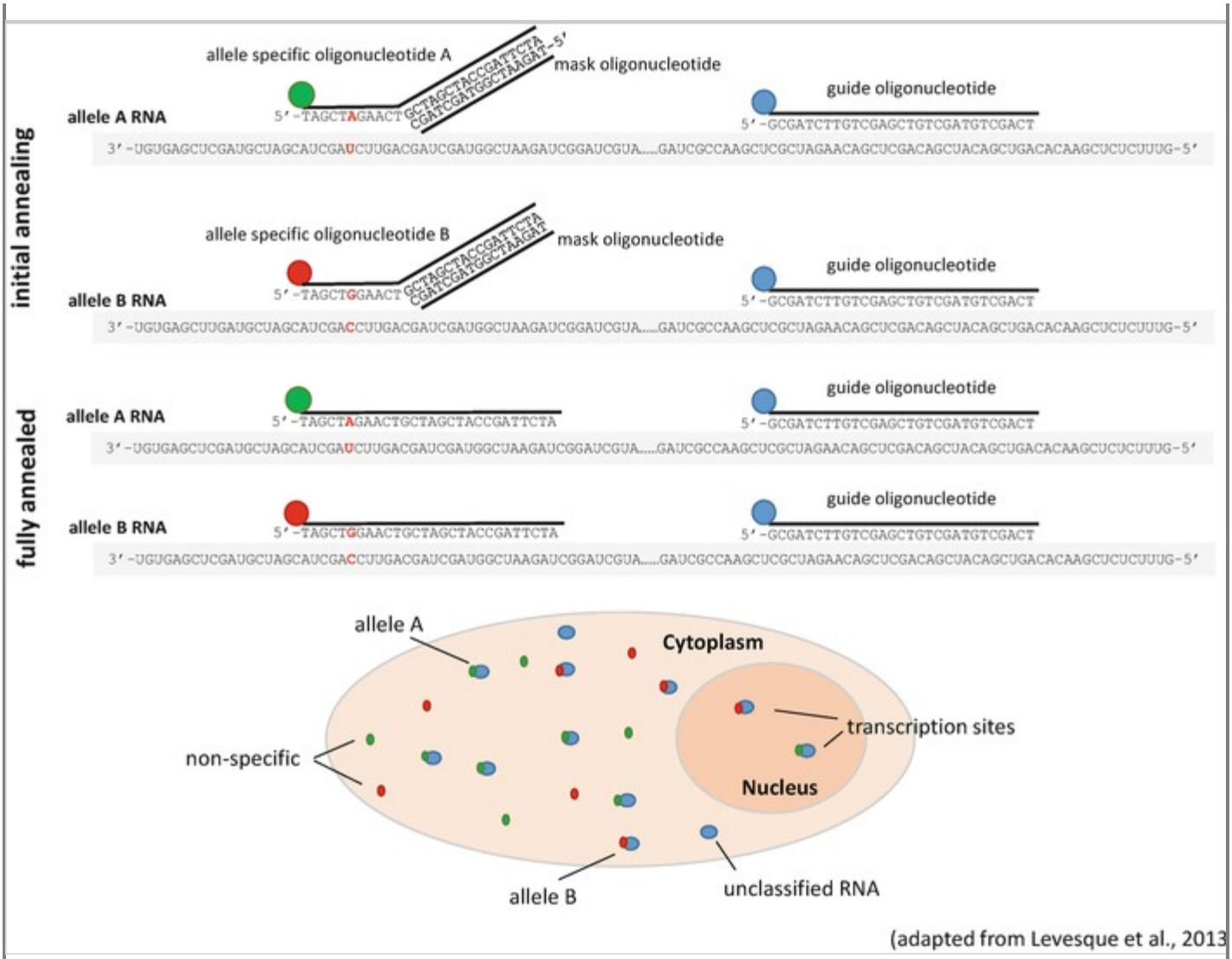

(adapted from Levesque et al., 2013

Another technique used to visualize the imprinted expression of genes in tissues is RNAscope in situ hybridization. Bonthuis and colleagues (Bonthuis et al. 2015) adapted the standard RNAscope (Advanced Cell Diagnostics, ACD) method to investigate actively transcribed alleles of specific genes in individual cell nuclei of fixed sections from the hypothalamic arcuate nucleus and dorsal raphe nucleus (Bonthuis et al. 2015). Using intronic oligonucleotide probes, which detect nascent transcripts in the nucleus before splicing occurs, they were able to determine through imaging for the presence of one or two hybridization signals ("color substrate dots") within a nucleus, whether one or both alleles of a gene were expressed. In contrast to the SNP-FISH technique, however, the RNAscope method does not provide information on the parental origin of monoallelic expression. Also, when used on tissue sections, the RNAscope approach has an inherent false detection rate problem, since the plane of sectioning might result in spatial separation of the two alleles in sequential sections. This would result in single hybridization signals within nuclei although biallelic expression occurs. This false detection rate needs to be accounted for by using appropriate control probes for biallelically expressed genes. The authors estimate that this method has an error rate of ~25% nuclei showing potentially false monoallelic expression (Bonthuis et al. 2015; Huang et al. 2017). Nevertheless, due to the high sensitivity of the hybridization probes and the straight-forward protocol, this approach can provide a useful first assessment of the localization of cells with mono- and biallelic expression within tissues. Especially since it can be combined with tissue RNAseq analysis (see below) for determination of parental expression biases.

Apart from these ~~in situ~~*in situ* techniques, molecular genetics approaches have been established to analyze epigenetic features as well as RNA expression from single-cell extracts (Angermueller et al. 2016; Cheow et al. 2015; Clark et al. 2018; Deng et al. 2014; Kelsey et al. 2017). Some methods are designed for a low-cost, focused investigation of specific loci (Cheow et al. 2015), while recent trends favor genome-wide next-generation sequencing technologies. RNAseq was first applied by Deng and colleagues (Deng et al. 2014) to investigate transcriptome-wide allelic expression in single cells using suitable strain-specific SNPs. Apart from parent-of-origin-dependent (imprinted) gene expression, they observed that a substantial proportion of genes (12–24%) are expressed monoallelically in a dynamic, random, and stochastic way (Deng et al. 2014). The most recent technological advances enable a combined analysis of DNA methylation, transcriptome, and nucleosome accessibility from single cells (scM&T-seq, scNMT-seq) (Angermueller et al. 2016; Kelsey et al. 2017). These approaches allow direct correlations to be made between epigenetic status, chromatin accessibility, and gene expression in a single cell. Although we cannot cover these methods in detail here [for a comprehensive review see Kelsey et al. (2017)], we would like to emphasize that consideration needs to be given to the way single cells can be isolated and the overall number of cells required for analysis. Most frequently, flow cytometry/fluorescence-activated cell sorting (FACS) is used to obtain single cells or nuclei (Luo et al. 2017), although microfluidics or manual collection via micromanipulators can also be applied depending on the tissue or cell type of interest (Cheow et al. 2015). Furthermore, and again depending on the complexity of the tissue to be investigated, usually hundreds or thousands of cells need to be included in an experiment to obtain a representative dataset for the cell population in question. As single-cell RNAseq and methylome analyses have already been applied on some brain regions (Luo et al. 2017; Tasic et al. 2016; Zeisel et al. 2015), it will be exciting to see the multi-omics approaches being adapted to neurobiological questions and specifically to characterize the large diversity of hypothalamic cell types in the future.

10.5. Perspectives

Within the brain, the hypothalamus has emerged as a major region in which imprinted genes are expressed. Here, they exert crucial functions in the regulation of postnatal development, energy homeostasis, hypothalamus–pituitary, and hypothalamus–thyroid neuroendocrine axes, as well as circadian rhythmicity and sleep. It is highly likely that the list provided in this chapter will be expanded in the near future, as several additional imprinted genes have been associated with a role in the hypothalamus, for example, *Neuronatin*, *Mkrn3*, *Grb10,* and *Liz.* On a molecular level, the recent developments in single-cell techniques will shed further light on the epigenetic regulation of imprinted genes. Many genes display an expression bias toward one parental allele when analyzed on a whole-tissue level. To clarify whether this is due to a mixture of cell types, some of which showing biallelic others monoallelic expression, and to understand the neurobiological relevance of this, will be an exciting field of future research.

Acknowledgment

We would like to thank the Wellcome Trust PhD studentship program in Cellular and Molecular Physiology at the University of Liverpool (099795/Z/12/Z) for research support.

10.6. Key References

AQ6

Buiting et al. (2016). This review provides an excellent overview about the clinical symptoms and genetics of Angelman syndrome.

Cassidy et al. (2012). A recommended review summarising the clinical symptoms as well as the genetics of Prader-Willi syndrome.

Chen et al. (2009). This paper shows for the first time genomic imprinting of *Gnas* in the brain and that loss of maternal allele-specific expression of Gnas in the brain is the cause for an obesity phenotype due to reduced energy expenditure.

Ferguson-Smith (2011) This review provides an excellent overview about the history of genomic imprinting research and well-studied imprinted genes clusters.

Kelsey et al. (2017). This recent review gives a good introduction into novel single-cell analysis techniques for epigenetics and gene expression.

Perez et al. (2015) This paper systematically analyzed imprinted gene expression within the brain transcriptome with excellent detail.

Peters (2014). This review emphasizes the physiological functions of imprinted genes.

Plagge et al. (2004). This paper identified the physiological functions of the paternally expressed transcript variant *Gnasxl* of the *Gnas* locus.

References

AQ7

Angermueller C, Clark SJ, Lee HJ, Macaulay IC, Teng MJ, Hu TX, Krueger F, Smallwood S, Ponting CP, Voet T, Kelsey G, Stegle O, Reik W (2016) Parallel single-cell sequencing links transcriptional and epigenetic heterogeneity. Nat Methods 13:229–232

Babak T, DeVeale B, Tsang EK, Zhou Y, Li X, Smith KS, Kukurba KR, Zhang R, Li JB, van der Kooy D, Montgomery SB, Fraser HB (2015) Genetic conflict reflected in tissue-specific maps of genomic imprinting in human and mouse. Nat Genet 47:544–549

Bartolomei MS, Ferguson-Smith AC (2011) Mammalian genomic imprinting. Cold Spring Harb Perspect Biol 3:a002592

Bieth E, Eddiry S, Gaston V, Lorenzini F, Buffet A, Conte Auriol F, Molinas C, Cailley D, Rooryck C, Arveiler B, Cavaille J, Salles JP, Tauber M (2015) Highly restricted deletion of the SNORD116 region is implicated in Prader-Willi Syndrome. Eur J Hum Genet 23:252–255

Bischof JM, Stewart CL, Wevrick R (2007) Inactivation of the mouse Magel2 gene results in growth abnormalities similar to Prader-Willi syndrome. Hum Mol Genet 16:2713–2719

Bonthuis PJ, Huang WC, Stacher Horndli CN, Ferris E, Cheng T, Gregg C (2015) Noncanonical genomic imprinting effects in offspring. Cell Rep 12:979–991

Cassidy SB, Schwartz S, Miller JL, Driscoll DJ (2012) Prader-Willi syndrome. Genet Med 14:10–26

Cavaille J (2017) Box C/D small nucleolar RNA genes and the Prader-Willi syndrome: a complex interplay. Wiley Interdiscip Rev RNA 8:e1417

Chen M, Wang J, Dickerson KE, Kelleher J, Xie T, Gupta D, Lai EW, Pacak K, Gavrilova O, Weinstein LS (2009) Central nervous system imprinting of the G protein G(s)α and its role in metabolic regulation. Cell Metab 9:548–555

Chen M, Nemechek NM, Mema E, Wang J, Weinstein LS (2011) Effects of deficiency of the G protein Gsα on energy and glucose homeostasis. Eur J Pharmacol 660:119–124

Chen M, Berger A, Kablan A, Zhang J, Gavrilova O, Weinstein LS (2012) Gsα deficiency in the paraventricular nucleus of the hypothalamus partially contributes to obesity associated with Gsα mutations. Endocrinology 153:4256–4265

Chen M, Shrestha YB, Podyma B, Cui Z, Naglieri B, Sun H, Ho T, Wilson EA, Li YQ, Gavrilova O, Weinstein LS (2017) Gsα deficiency in the dorsomedial hypothalamus underlies obesity associated with Gsα mutations. J Clin Invest 127:500–510

Cheow LF, Quake SR, Burkholder WF, Messerschmidt DM (2015) Multiplexed locus-specific analysis of DNA methylation in single cells. Nat Protoc 10:619–631

Clark SJ, Argelaguet R, Kapourani CA, Stubbs TM, Lee HJ, Alda-Catalinas C, Krueger F, Sanguinetti G, Kelsey G, Marioni JC, Stegle O, Reik W (2018) scNMT-seq enables joint profiling of chromatin accessibility DNA methylation and transcription in single cells. Nat Commun 9:781

Curley JP, Pinnock SB, Dickson SL, Thresher R, Miyoshi N, Surani MA, Keverne EB (2005) Increased body fat in mice with a targeted mutation of the paternally expressed imprinted gene Peg3. FASEB J 19:1302–1304

Dauber A, Cunha-Silva M, Macedo DB, Brito VN, Abreu AP, Roberts SA, Montenegro LR, Andrew M, Kirby A, Weirauch MT, Labilloy G, Bessa DS, Carroll RS, Jacobs DC, Chappell PE, Mendonca BB, Haig D, Kaiser UB, Latronico AC (2017) Paternally inherited DLK1 deletion associated with familial central precocious puberty. J Clin Endocrinol Metab 102:1557–1567

Dejeux E, El abdalaoui H, Gut IG, Tost J (2009) Identification and quantification of differentially methylated loci by the pyrosequencing technology. Methods Mol Biol 507:189–205

Deng Q, Ramskold D, Reinius B, Sandberg R (2014) Single-cell RNA-seq reveals dynamic, random monoallelic gene expression in mammalian cells. Science 343:193–196

Denizot AL, Besson V, Correra RM, Mazzola A, Lopes I, Courbard JR, Marazzi G, Sassoon DA (2016) A novel mutant allele of Pw1/Peg3 does not affect maternal behavior or nursing behavior. PLoS Genet 12:e1006053

Ding F, Li HH, Zhang S, Solomon NM, Camper SA, Cohen P, Francke U (2008) SnoRNA Snord116 (Pwcr1/MBII-85) deletion causes growth deficiency and hyperphagia in mice. PLoS One 3:e1709

Eads CA, Laird PW (2002) Combined bisulfite restriction analysis (COBRA). Methods Mol Biol 200:71–85

Ehlen JC, Jones KA, Pinckney L, Gray CL, Burette S, Weinberg RJ, Evans JA, Brager AJ, Zylka MJ, Paul KN,

Philpot BD, DeBruyne JP (2015) Maternal Ube3a loss disrupts sleep homeostasis but leaves circadian rhythmicity largely intact. J Neurosci 35:13587–13598

Ferguson-Smith AC (2011) Genomic imprinting: the emergence of an epigenetic paradigm. Nat Rev Genet 12:565–575

Ferron SR, Charalambous M, Radford E, McEwen K, Wildner H, Hind E, Morante-Redolat JM, Laborda J, Guillemot F, Bauer SR, Farinas I, Ferguson-Smith AC (2011) Postnatal loss of Dlk1 imprinting in stem cells and niche astrocytes regulates neurogenesis. Nature 475:381–385

Genevieve D, Sanlaville D, Faivre L, Kottler ML, Jambou M, Gosset P, Boustani-Samara D, Pinto G, Ozilou C, Abeguile G, Munnich A, Romana S, Raoul O, Cormier-Daire V, Vekemans M (2005) Paternal deletion of the GNAS imprinted locus (including Gnasxl) in two girls presenting with severe pre- and post-natal growth retardation and intractable feeding difficulties. Eur J Hum Genet 13:1033–1039

Gerard M, Hernandez L, Wevrick R, Stewart CL (1999) Disruption of the mouse necdin gene results in early post-natal lethality. Nat Genet 23:199–202

Ginart P, Kalish JM, Jiang CL, Yu AC, Bartolomei MS, Raj A (2016) Visualizing allele-specific expression in single cells reveals epigenetic mosaicism in an H19 loss-of-imprinting mutant. Genes Dev 30:567–578

Haig D (2004) Genomic imprinting and kinship: how good is the evidence? Annu Rev Genet 38:553–585

Harris RA, Wang T, Coarfa C, Nagarajan RP, Hong C, Downey SL, Johnson BE, Fouse SD, Delaney A, Zhao Y, Olshen A, Ballinger T, Zhou X, Forsberg KJ, Gu J, Echipare L, O'Geen H, Lister R, Pelizzola M, Xi Y, Epstein CB, Bernstein BE, Hawkins RD, Ren B, Chung WY, Gu H, Bock C, Gnirke A, Zhang MQ, Haussler D, Ecker JR, Li W, Farnham PJ, Waterland RA, Meissner A, Marra MA, Hirst M, Milosavljevic A, Costello JF (2010) Comparison of sequencing-based methods to profile DNA methylation and identification of monoallelic epigenetic modifications. Nat Biotechnol 28:1097–1105

Hasegawa K, Kawahara T, Fujiwara K, Shimpuku M, Sasaki T, Kitamura T, Yoshikawa K (2012) Necdin controls Foxo1 acetylation in hypothalamic arcuate neurons to modulate the thyroid axis. J. Neurosci 32:5562–5572

He Q, Zhu Y, Corbin BA, Plagge A, Bastepe M (2015) The G protein alpha subunit variant XLαs promotes inositol 1,4,5-trisphosphate signaling and mediates the renal actions of parathyroid hormone in vivo. Sci Signal 8:ra84

Huang WC, Ferris E, Cheng T, Horndli CS, Gleason K, Tamminga C, Wagner JD, Boucher KM, Christian JL, Gregg C (2017) Diverse non-genetic, allele-specific expression effects shape genetic architecture at the cellular level in the mammalian brain. Neuron 93:1094–1109

Ivanova E, Kelsey G (2011) Imprinted genes and hypothalamic function. J Mol Endocrinol 47:R67–R74

Kawashima S, Nakamura A, Inoue T, Matsubara K, Horikawa R, Wakui K, Takano K, Fukushima Y, Tatematsu T, Mizuno S, Tsubaki J, Kure S, Matsubara Y, Ogata T, Fukami M, Kagami M (2018) Maternal uniparental disomy for chromosome 20: physical and endocrinological characteristics of five patients. J Clin Endocrinol Metab 103:2083–2088

Kelsey G, Stegle O, Reik W (2017) Single-cell epigenomics: recording the past and predicting the future. Science 358:69–75

Kozlov SV, Bogenpohl JW, Howell MP, Wevrick R, Panda S, Hogenesch JB, Muglia LJ, Van Gelder RN, Herzog ED, Stewart CL (2007) The imprinted gene Magel2 regulates normal circadian output. Nat Genet 39:1266–1272

Krechowec SO, Burton KL, Newlaczyl AU, Nunn N, Vlatkovic N, Plagge A (2012) Postnatal changes in the expression pattern of the imprinted signalling protein XLαs underlie the changing phenotype of deficient mice. PLoS One 7:e29753

LaSalle JM, Reiter LT, Chamberlain SJ (2015) Epigenetic regulation of UBE3A and roles in human neurodevelopmental disorders. Epigenomics 7:1213–1228

Lee S, Walker CL, Karten B, Kuny SL, Tennese AA, O'Neill MA, Wevrick R (2005) Essential role for the Prader-Willi syndrome protein necdin in axonal outgrowth. Hum Mol Genet 14:627–637

Levesque MJ, Ginart P, Wei Y, Raj A (2013) Visualizing SNVs to quantify allele-specific expression in single cells. Nat Methods 10:865–867

Li L, Keverne EB, Aparicio SA, Ishino F, Barton SC, Surani MA (1999) Regulation of maternal behavior and offspring growth by paternally expressed Peg3. Science 284:330–333

Li YQ, Shrestha Y, Pandey M, Chen M, Kablan A, Gavrilova O, Offermanns S, Weinstein LS (2016) G(q/11)α and G(s)α mediate distinct physiological responses to central melanocortins. J Clin Invest 126:40–49

Luo C, Keown CL, Kurihara L, Zhou J, He Y, Li J, Castanon R, Lucero J, Nery JR, Sandoval JP, Bui B, Sejnowski TJ, Harkins TT, Mukamel EA, Behrens MM, Ecker JR (2017) Single-cell methylomes identify neuronal subtypes and regulatory elements in mammalian cortex. Science 357:600–604

Lyko F (2018) The DNA methyltransferase family: a versatile toolkit for epigenetic regulation. Nat Rev Genet 19:81–92

Maillard J, Park S, Croizier S, Vanacker C, Cook JH, Prevot V, Tauber M, Bouret SG (2016) Loss of Magel2 impairs the development of hypothalamic Anorexigenic circuits. Hum Mol Genet 25:3208–3215

Mantovani G, Bastepe M, Monk D, de Sanctis L, Thiele S, Usardi A, Ahmed SF, Bufo R, Choplin T, De Filippo G, Devernois G, Eggermann T, Elli FM, Freson K, Garcia Ramirez A, Germain-Lee EL, Groussin L, Hamdy N, Hanna P, Hiort O, Juppner H, Kamenicky P, Knight N, Kottler ML, Le Norcy E, Lecumberri B, Levine MA, Makitie O, Martin R, Martos-Moreno GA, Minagawa M, Murray P, Pereda A, Pignolo R, Rejnmark L, Rodado R, Rothenbuhler A, Saraff V, Shoemaker AH, Shore EM, Silve C, Turan S, Woods P, Zillikens MC, Perez de Nanclares G, Linglart A (2018) Diagnosis and management of pseudohypoparathyroidism and related disorders: first international Consensus Statement. Nat Rev Endocrinol 14:476–500

Martinez ME, Charalambous M, Saferali A, Fiering S, Naumova AK, Germain DS, Ferguson-Smith AC, Hernandez A (2014) Genomic imprinting variations in the mouse type 3 deiodinase gene between tissues and brain regions. Mol Endocrinol 28:1875–1886

Matarazzo V, Caccialupi L, Schaller F, Shvarev Y, Kourdougli N, Bertoni A, Menuet C, Voituron N, Deneris E, Gaspar P, Bezin L, Durbec P, Hilaire G, Muscatelli F (2017) Necdin shapes serotonergic development and SERT activity modulating breathing in a mouse model for Prader-Willi syndrome. elife 6:e32640

Mehta S, Williamson CM, Ball S, Tibbit C, Beechey C, Fray M, Peters J (2015) Transcription driven somatic DNA methylation within the imprinted Gnas cluster. PLoS One 10:e0117378

Meister B, Perez-Manso M, Daraio T (2013) Delta-like 1 homologue is a hypothalamus- enriched protein that is present in orexin-containing neurones of the lateral hypothalamic area. J Neuroendocrinol 25:617–625

Mercer RE, Michaelson SD, Chee MJ, Atallah TA, Wevrick R, Colmers WF (2013) Magel2 is required for leptin-mediated depolarization of POMC neurons in the hypothalamic arcuate nucleus in mice. PLoS Genet 9:e1003207

Miller NL, Wevrick R, Mellon PL (2009) Necdin, a Prader-Willi syndrome candidate gene, regulates gonadotropin-releasing hormone neurons during development. Hum Mol Genet 18:248–260

Mulchandani S, Bhoj EJ, Luo M, Powell-Hamilton N, Jenny K, Gripp KW, Elbracht M, Eggermann T, Turner CL, Temple IK, Mackay DJ, Dubbs H, Stevenson DA, Slattery L, Zackai EH, Spinner NB, Krantz ID, Conlin LK (2016) Maternal uniparental disomy of chromosome 20: a novel imprinting disorder of growth failure. Genet Med 18:309–315

Muscatelli F, Abrous DN, Massacrier A, Boccaccio I, Le Moal M, Cau P, Cremer H (2000) Disruption of the mouse Necdin gene results in hypothalamic and behavioral alterations reminiscent of the human Prader-Willi syndrome. Hum Mol Genet 9:3101–3110

Nunn N, Feetham CH, Martin J, Barrett-Jolley R, Plagge A (2013) Elevated blood pressure, heart rate and body temperature in mice lacking the XLαs protein of the Gnas locus is due to increased sympathetic tone. Exp Physiol 98:1432–1445

Olova N, Krueger F, Andrews S, Oxley D, Berrens RV, Branco MR, Reik W (2018) Comparison of whole-genome bisulfite sequencing library preparation strategies identifies sources of biases affecting DNA methylation data. Genome Biol 19:33

Perez JD, Rubinstein ND, Fernandez DE, Santoro SW, Needleman LA, Ho-Shing O, Choi JJ, Zirlinger M, Chen SK, Liu JS, Dulac C (2015) Quantitative and functional interrogation of parent-of-origin allelic expression biases in the brain. elife 4:e07860

Peters J (2014) The role of genomic imprinting in biology and disease: an expanding view. Nat Rev Genet 15:517–530

Plagge A (2012) Non-coding RNAs at the Gnas and Snrpn-Ube3a imprinted gene loci and their involvement in hereditary disorders. Front Genet 3:264

Plagge A, Gordon E, Dean W, Boiani R, Cinti S, Peters J, Kelsey G (2004) The imprinted signaling protein XLαs is required for postnatal adaptation to feeding. Nat Genet 36:818–826

Plagge A, Isles AR, Gordon E, Humby T, Dean W, Gritsch S, Fischer-Colbrie R, Wilkinson LS, Kelsey G (2005)

Imprinted Nesp55 influences behavioral reactivity to novel environments. Mol Cell Biol 25:3019–3026

Plasschaert RN, Bartolomei MS (2014) Genomic imprinting in development, growth, behavior and stem cells. Development 141:1805–1813

Podyma B, Sun H, Wilson EA, Carlson B, Pritikin E, Gavrilova O, Weinstein LS, Chen M (2018) The stimulatory G protein Gsα is required in melanocortin 4 receptor-expressing cells for normal energy balance, thermogenesis, and glucose metabolism. J Biol Chem 293:10993–11005

Polex-Wolf J, Lam BY, Larder R, Tadross J, Rimmington D, Bosch F, Cenzano VJ, Ayuso E, Ma MK, Rainbow K, Coll AP, O'Rahilly S, Yeo GS (2018) Hypothalamic loss of Snord116 recapitulates the hyperphagia of Prader-Willi syndrome. J Clin Invest 128:960–969

Richard N, Molin A, Coudray N, Rault-Guillaume P, Juppner H, Kottler ML (2013) Paternal GNAS mutations lead to severe intrauterine growth retardation (IUGR) and provide evidence for a role of XLαs in fetal development. J Clin Endocrinol Metab 98:E1549–E1556

Schaller F, Watrin F, Sturny R, Massacrier A, Szepetowski P, Muscatelli F (2010) A single postnatal injection of oxytocin rescues the lethal feeding behaviour in mouse newborns deficient for the imprinted Magel2 gene. Hum Mol Genet 19:4895–4905

Shi SQ, Bichell TJ, Ihrie RA, Johnson CH (2015) Ube3a imprinting impairs circadian robustness in Angelman syndrome models. Curr Biol 25:537–545

Skryabin BV, Gubar LV, Seeger B, Pfeiffer J, Handel S, Robeck T, Karpova E, Rozhdestvensky TS, Brosius J (2007) Deletion of the MBII-85 snoRNA gene cluster in mice results in postnatal growth retardation. PLoS Genet 3:e235

Stohn JP, Martinez ME, Zafer M, Lopez-Espindola D, Keyes LM, Hernandez A (2018) Increased aggression and lack of maternal behavior in Dio3-deficient mice are associated with abnormalities in oxytocin and vasopressin systems. Genes Brain Behav 17:23–35

Tacer KF, Potts PR (2017) Cellular and disease functions of the Prader-Willi Syndrome gene MAGEL2. Biochem J 474:2177–2190

Tasic B, Menon V, Nguyen TN, Kim TK, Jarsky T, Yao Z, Levi B, Gray LT, Sorensen SA, Dolbeare T, Bertagnolli D, Goldy J, Shapovalova N, Parry S, Lee C, Smith K, Bernard A, Madisen L, Sunkin SM, Hawrylycz M, Koch C, Zeng H (2016) Adult mouse cortical cell taxonomy revealed by single cell transcriptomics. Nat Neurosci 19:335–346

Tommiska J, Kansakoski J, Skibsbye L, Vaaralahti K, Liu X, Lodge EJ, Tang C, Yuan L, Fagerholm R, Kanters JK, Lahermo P, Kaunisto M, Keski-Filppula R, Vuoristo S, Pulli K, Ebeling T, Valanne L, Sankila EM, Kivirikko S, Laaperi M, Casoni F, Giacobini P, Phan- Hug F, Buki T, Tena-Sempere M, Pitteloud N, Veijola R, Lipsanen-Nyman M, Kaunisto K, Mollard P, Andoniadou CL, Hirsch JA, Varjosalo M, Jespersen T, Raivio T (2017) Two missense mutations in KCNQ1 cause pituitary hormone deficiency and maternally inherited gingival fibromatosis. Nat Commun 8:1289

Turan S, Bastepe M (2013) The GNAS complex locus and human diseases associated with loss-of-function

mutations or epimutations within this imprinted gene. Horm Res Paediatr 80:229–241

Villanueva C, Jacquier S, de Roux N (2012) DLK1 is a somato-dendritic protein expressed in hypothalamic arginine-vasopressin and oxytocin neurons. PLoS One 7:e36134

Weinstein LS (2014) Role of G(s)α in central regulation of energy and glucose metabolism. Horm Metab Res 46:841–844

Wijesuriya TM, De Ceuninck L, Masschaele D, Sanderson MR, Carias KV, Tavernier J, Wevrick R (2017) The Prader-Willi syndrome proteins MAGEL2 and necdin regulate leptin receptor cell surface abundance through ubiquitination pathways. Hum Mol Genet 26:4215–4230

Wu Z, Martinez ME, St Germain DL, Hernandez A (2017) Type 3 deiodinase role on central thyroid hormone action affects the leptin-melanocortin system and circadian activity. Endocrinology 158:419–430

Xie T, Plagge A, Gavrilova O, Pack S, Jou W, Lai EW, Frontera M, Kelsey G, Weinstein LS (2006) The alternative stimulatory G protein α-subunit XLαs is a critical regulator of energy and glucose metabolism and sympathetic nerve activity in adult mice. J Biol Chem 281:18989–18999

Zeisel A, Munoz-Manchado AB, Codeluppi S, Lonnerberg P, La Manno G, Jureus A, Marques S, Munguba H, He L, Betsholtz C, Rolny C, Castelo-Branco G, Hjerling-Leffler J, Linnarsson S (2015) Brain structure. Cell types in the mouse cortex and hippocampus revealed by single-cell RNA-seq. Science 347:1138–1142

Buiting K, Williams C, Horsthemke B, (2016) Angelman syndrome — insights into a rare neurogenetic disorder. Nat Rev Neurol 12 (10):584-593